Proceedings of the 41st IEEE
Conference on Decision and Control
Las Vegas, Nevada USA, December 2002

Identification of an Electromagnetic Actuator*

Seth L. Lacy Dennis S. Bernstein†

Abstract

We apply time-domain system identification techniques to an electromagnetic actuator. This actuator is part of the vibration isolation testbed at the University of Michigan.

1 Introduction

Nonlinear system identification remains one of the most challenging and potentially useful problem areas in system theory. Numerous approaches have been developed for this problem, including black box [1, 5, 7–9, 17, 24] and gray box techniques [2–4, 6, 8, 10–23, 25–32].

Black box methods make little or no assumptions concerning the structure of the system. Gray box or *block-structured* identification involves the interconnection of two types of input-output blocks. The first type of block is a linear dynamic system, for example $y = G(q^{-1})u$, while the second type is a static nonlinearity, for example $y = u^2$. The gray box case includes the identification of block-structured models, such as the classical Hammerstein model (linear system with input nonlinearity), Wiener model (linear system with output nonlinearity), and nonlinear feedback model (linear system with a nonlinearity in feedback). Block-structured identification provides physically meaningful engineering models of the system components but requires prior knowledge of the system structure.

We apply system identification methods to a linear motor used in the active vibration isolation testbed at the University of Michigan, see Figure 1. The isolator is a six degree of freedom Stuart platform consisting of a lower base platform, six struts, and an upper platform for mounting equipment.The struts incorporate permanent magnet/voice coil linear actuators, Kimco model LA25-42-012Z, with a total stroke of about one inch.The permanent magnets are mounted to the base plate with a universal joint. The coil is connected to the upper plate with a universal joint. The rod/coil subsystem moves relative to the permanent magnet on linear bearings. The entire permanent magnet/voice coil linear motor is enclosed in a cylinder with slots for access to the capacitive displacement sensor and voice coil. The enclosure cylinder is air cooled to dissipate the heat produced by the coil, which has a resistance of about 2.2 Ohms. The capacitive sensor is mounted at the top of the can and measures the capacitance between itself and the top of the voice coil, which can then be mapped to relative displacement. An accelerometer is mounted at the top end of the moving rod, just below the universal joint.

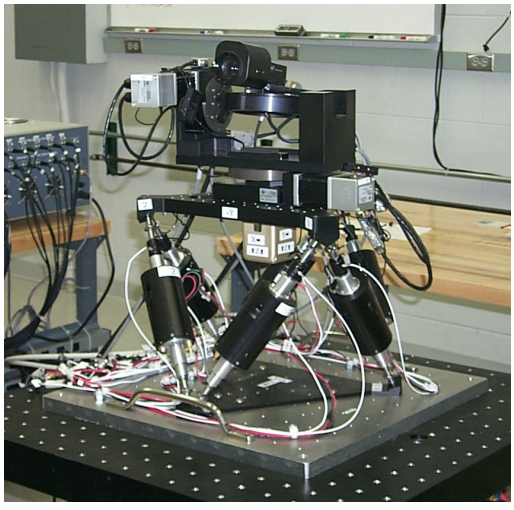

Figure 1: Camera, Azimuth-Elevation Stage, Isolation Stage, and Top of Shaker

The control input to the strut is the current in the voice coil. We measure position with a capacitive displacement sensor, Capacitec model HPB-500A-A-L2-5-B-D. This sensor is approximately linear for displacements less than about 0.25 inches, but is nonlinear for displacements beyond 0.25 inches. We measure acceleration with a single axis accelerometer, Kistler model 8636C10, that has a range of ± 10 g with peak readings at ± 16 g and shock tolerance of $\pm 10,000$ g for 0.2 ms.

We mounted the struts vertically in a test jig and collected step response data as well as dynamic response data, see Figure 2. We use several identification schemes to identify the linear and nonlinear dynamics of the strut. For identification, we have access to three signals, the current input $u(t)$, the capacitive displacement measurement $y(t)$, and the acceleration measurement $a(t)$.

2 Sensor Noise

We collected sixteen seconds of data at 1 kHz with constant input and the cooling air turned off. This allows us to estimate the covariance matrix of the sensor

*Supported in part by NASA under GSRP NGT4-52421 and AFOSR under grant F49620-01-1-0094.

†Aerospace Engineering Department, University of Michigan, Ann Arbor MI 48109, {sethlacy,dsbaero}@umich.edu

Figure 2: The strut identification test jig

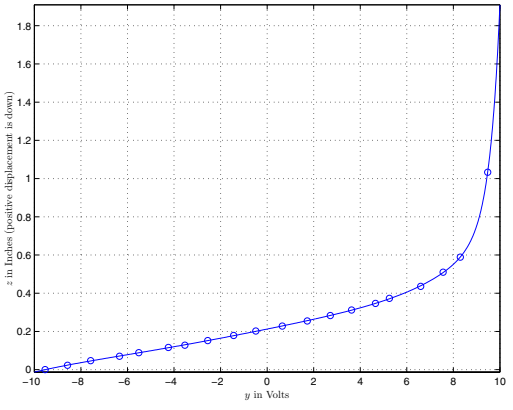

Figure 3: Displacement nonlinearity, $z = p^{-1}(y)$

noise (in volts^2)

$$\hat{R} = 10^{-6} \begin{bmatrix} 0.8438 & -0.0022 \\ -0.0022 & 0.4435 \end{bmatrix}. \quad (2.1)$$

We can then calculate the effective resolutions of our sensors in bits as

$$r_y = \log_2(20/\sigma_y) = \log_2(20/\sqrt{\hat{R}_{11}}) = 14.4102 \quad (2.2)$$

for the capacitive sensor, and

$$r_a = \log_2(20/\sigma_a) = \log_2(20/\sqrt{\hat{R}_{22}}) = 14.8742 \quad (2.3)$$

for the accelerometer. Our A/D converters have a range of ± 10 volts and a resolution of 16 bits. With the cooling air off, we have only lost between one and two bits of resolution to noise.

3 Static Experiments

We calibrated the capacitive sensor $y = p(z)$ using calipers, see Figure 3, where y is the measured output in volts, and z is the true displacement in inches. To estimate the coefficients x, We numerically optimized a nonlinear least-squares cost function in the variable x_9,

$$J(x_9) \triangleq \left(\sum_i \left(z(i) - \left(x_8 e^{x_9 y(i)} + x_1 + x_2 y(i) + x_3 y^2(i) + x_4 y^3(i) + x_5 y^4(i) + x_6 y^5(i) + x_7 y^6(i) \right) \right)^2 \right)^{1/2}, \quad (3.1)$$

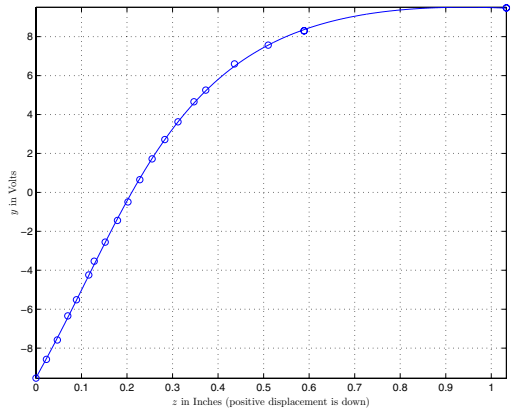

Figure 4: Displacement nonlinearity, $y = p(z)$

$$\begin{bmatrix} x_1 \\ x_2 \\ x_3 \\ x_4 \\ x_5 \\ x_6 \\ x_7 \\ x_8 \end{bmatrix}^{\mathrm{T}} \triangleq \begin{bmatrix} z(1) & \cdots & z(N) \end{bmatrix} \begin{bmatrix} 1 & \cdots & 1 \\ y(1) & \cdots & y(N) \\ y^2(1) & \cdots & y^2(N) \\ y^3(1) & \cdots & y^3(N) \\ y^4(1) & \cdots & y^4(N) \\ y^5(1) & \cdots & y^5(N) \\ y^6(1) & \cdots & y^6(N) \\ e^{x_9 y(1)} & \cdots & e^{x_9 y(N)} \end{bmatrix}^{\mathrm{R}}. \quad (3.2)$$

We obtain

$$p^{-1}(y) \approx x_1 + x_2 y + x_3 y^2 + x_4 y^3 + x_5 y^4 + x_6 y^5 + x_7 y^6 + x_8 e^{x_9 y}, \quad (3.3)$$

where

$$x \triangleq \begin{bmatrix} 0.2125 & 0.02464 & 0.4003e-3 \\ 0.2968e-4 & 0.1083e-4 & 0.1215e-5 \\ 0.2391e-7 & 0.7538e-10 & 2.3428 \end{bmatrix}^{\mathrm{T}}. \quad (3.4)$$

We also calibrated p, see Figure 4. To estimate the coefficients x, we numerically optimized a nonlinear least-squares cost function in the variables x_5 and x_6,

$$J(x_5, x_6) \triangleq \Big(\sum_i \big(y(i) - (x_1 + x_2 z(i)^{1/2} + x_3 z(i) + x_4 \arctan(x_5 + x_6 z(i))) \big)^2 \Big)^{1/2}, \quad (3.5)$$

$$\begin{bmatrix} x_1 \\ x_2 \\ x_3 \\ x_4 \end{bmatrix}^{\mathrm{T}} \triangleq \begin{bmatrix} y(1) & \cdots & y(N) \end{bmatrix} \times \begin{bmatrix} 1 & \cdots & 1 \\ \sqrt{z(1)} & \cdots & \sqrt{z(N)} \\ z(1) & \cdots & z(N) \\ \operatorname{atan}(x_5 + x_6 z(1)) & \cdots & \operatorname{atan}(x_5 + x_6 z(N)) \end{bmatrix}^{\mathrm{R}}. \quad (3.6)$$

We obtain

$$p(z) \approx x_1 + x_2 \sqrt{z} + x_3 z + x_4 \arctan(x_5 + x_6 z), \quad (3.7)$$

where

$$x \triangleq \begin{bmatrix} -3.9432 & 0.5482 & -5.7034 \\ 14.7234 & -0.4002 & 3.5410 \end{bmatrix}. \quad (3.8)$$

Now that we have used the static experiments to approximate the system output nonlinearity, we turn to dynamic experiments to identify the dynamics of the strut.

4 Dynamic Experiments

We collected sixteen seconds of data at a sampling rate of 1 kHz to obtain 16001 data points.We perform several identification experiments. For each experiment we use the first $\ell = 2^{13} = 8192$ data points for identification, and the last 7937 data points for validation. There is an overlap of $q = 128$ data points because we initialize the validation with the last state estimate from the identification, see [19]. We evaluate the identification results using the cost functions

$$J_y \triangleq \frac{\|y-\hat{y}\|}{\|y\|} = \left(\frac{\sum_{i=8065}^{16001}(y(i)-\hat{y}(i))^2}{\sum_{i=8065}^{16001} y(i)^2}\right)^{\frac{1}{2}}, \quad (4.1)$$

$$J_a \triangleq \frac{\|a-\hat{a}\|}{\|a\|} = \left(\frac{\sum_{i=8065}^{16001}(a(i)-\hat{a}(i))^2}{\sum_{i=8065}^{16001} a(i)^2}\right)^{\frac{1}{2}}, \quad (4.2)$$

where $\hat{y}$ and $\hat{a}$ are the position and acceleration predicted by the identified model.

4.1 Linear SIMO Model

Here we identify a linear model using measurements y and a of both the position z and acceleration $\ddot{z}$. The identification produced a linear model that approximates the true dynamics. We use the method described in [19] to identify an 8th order linear model

$$x(k+1) = Ax(k) + Bu(k), \quad (4.3)$$

$$\begin{bmatrix} y(k) \\ a(k) \end{bmatrix} = Cx(k) + Du(k). \quad (4.4)$$

To validate the identified model, We initialize the identified system with the final state of the identification data set, then drive both the true and identified system with the same input sequence and compare their response. The resulting costs are

$$J_y = 0.43824, \quad (4.5)$$

$$J_a = 0.18189, \quad (4.6)$$

indicating that we have fit the acceleration data better than we have fit the position data, presumably due to the nonlinear characteristic of the capacitive displacement sensor and different noise levels in the signals from the two sensors. The validation results are shown in Figure 5.

4.2 Linear SISO Model Using Only Position Measurements

Here we follow the same procedure as in the previous section, with the exception that we only allow measurements of the position y. we identify a 6th order model

$$x(k+1) = Ax(k) + Bu(k) \quad (4.7)$$

$$y(k) = Cx(k) + Du(k), \quad (4.8)$$

with validation cost

$$J_y = 0.58767, \quad (4.9)$$

indicating that we have lost performance with the loss of the acceleration sensor. The validation results are shown in Figure 6.

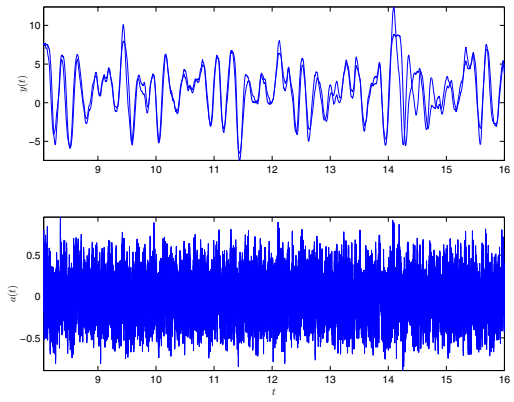

Figure 5: Validation Data: Thick Line Represents True Measured Data, Thin Line Represents Output of Identified System

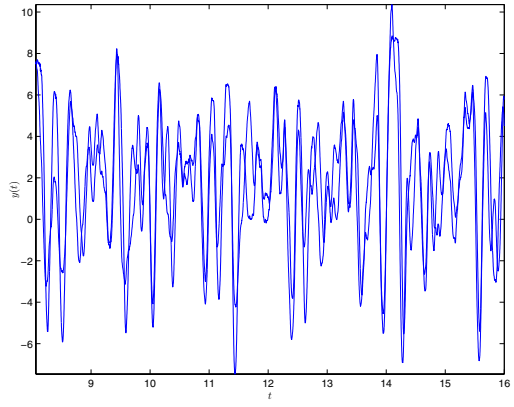

Figure 6: Validation Data: Thick Line Represents True Measured Data, Thin Line Represents Output of Identified System

4.3 Linear SISO Model Using Only Acceleration Measurements

Here we follow the same procedure as in the previous section, with the exception that we only allow measurements of the acceleration a. We identify a 4th order model

$$x(k+1) = Ax(k) + Bu(k) \quad (4.10)$$

$$a(k) = Cx(k) + Du(k), \quad (4.11)$$

with validation cost

$$J_a = 0.18996, \quad (4.12)$$

indicating that we have lost some performance with the loss of the position sensor. The validation results are shown in Figure 7.

4.4 Nonlinear SIMO Hammerstein Model

Here we identify a nonlinear Hammerstein model using the method of [19]. We allow measurements of

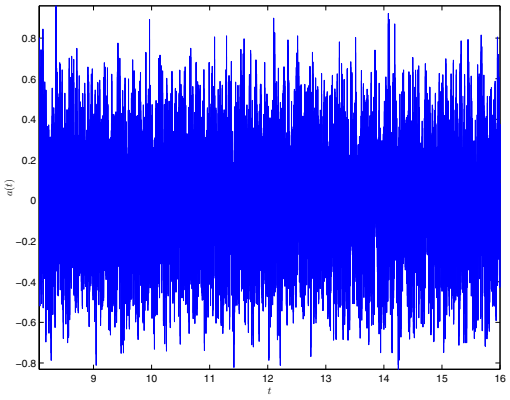

Figure 7: Validation Data: Thick Line Represents True Measured Data, Thin Line Represents Output of Identified System

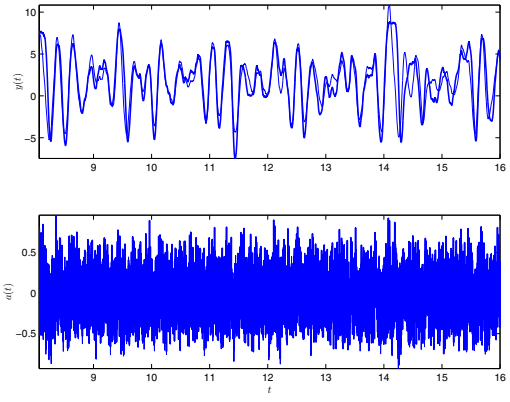

Figure 8: Validation Data: Thick Line Represents True Measured Data, Thin Line Represents Output of Identified System

both the position y and the acceleration a. We identify a 6th order model

$$x(k+1) = Ax(k) + B \begin{bmatrix} 1 \\ u(k) \\ u^2(k) \end{bmatrix} \tag{4.13}$$

$$\begin{bmatrix} y(k) \\ a(k) \end{bmatrix} = Cx(k) + D \begin{bmatrix} 1 \\ u(k) \\ u^2(k) \end{bmatrix}, \tag{4.14}$$

with validation costs

$$J_y = 0.47191, \tag{4.15}$$

$$J_a = 0.23115 \tag{4.16}$$

indicating that we have lost some performance compared to the linear identification. On the other hand, we also reduced the model order by two. The validation results are shown in Figure 8.

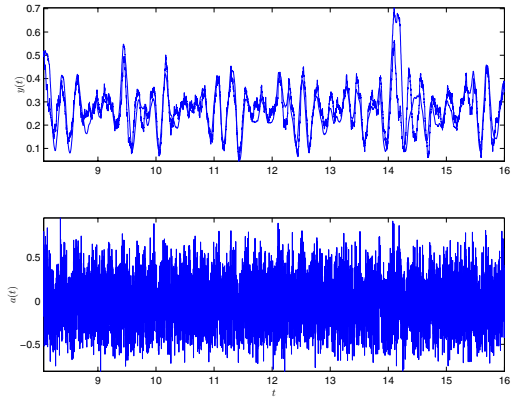

Figure 9: Validation Data: Thick Line Represents True Measured Data, Thin Line Represents Output of Identified System

4.5 Non-Linear Model Using Both Position and Acceleration Measurements and Knowledge of $p^{-1}(y)$

Here we identify a nonlinear Wiener model. We allow measurements of both the position y and the acceleration a, and calculate z using p^{-1}. We identify a 6th order model

$$x(k+1) = Ax(k) + Bu(k) \tag{4.17}$$

$$\begin{bmatrix} z(k) \\ a(k) \end{bmatrix} = Cx(k) + Du(k) \tag{4.18}$$

$$y(k) = p(z(k)) \tag{4.19}$$

with validation costs

$$J_y = 0.24138, \tag{4.20}$$

$$J_a = 0.96345 \tag{4.21}$$

indicating that we have lost performance in the acceleration transfer function, but improved the position transfer function! The validation results are shown in Figure 8.

4.6 Non-Linear Wiener Model Using Position

Here we identify a nonlinear Wiener model using measurements of position only using the method of [20]. We drive the system slowly at 10 Hz to reduce the memory requirements of the method. We collect 10 minutes of data at 10 Hz to obtain 6001 data points.We use the first 5800 data points for identification and the last 201 data points for validation.

We identify an FIR Wiener system with a polynomial nonlinearity,

$$z(k) = \sum_{i=0}^{21} h_i u(k-i), \tag{4.22}$$

$$y(k) = \sum_{i=0}^{3} c_i z(k)^i, \tag{4.23}$$

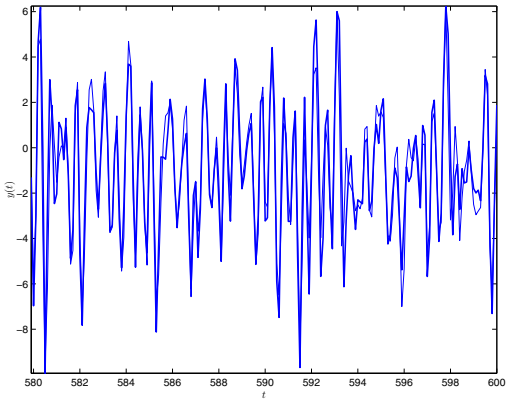

Figure 10: Validation Data: Thick Line Represents True Measured Data, Thin Line Represents Output of Identified System

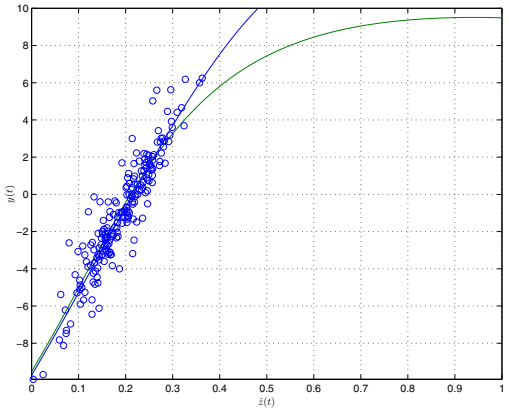

Figure 11: Output nonlinearity and calibration curve

where u is the measured input, z is the unmeasured intermediate signal, and y is the output of the capacitive sensor. We use the first SVD method of [20] to initialize the prediction error cost function, and obtain estimates $\hat{c}$ and $\hat{h}$, see Figure 10. The validation cost is

$$J_y = 0.3539, \tag{4.24}$$

indication improved performance over the linear models. After scaling (choosing $\sigma \neq 1$) we plot the output nonlinearity next to the calibration curve, see Figure 11 While the estimated nonlinearity does have some curvature in the correct direction, we miss much of the extreme curvature of the calibration data. Unfortunately, we were unable to collect much data in that region due to limited actuator authority in the high displacement region.

5 Conclusion

We calibrated our sensors to find that their effective resolutions are better than 14 bits, which indicates that they are pretty clean. In our dynamic identification experiments, we found that removing a sensor generally resulted in a lower order but less accurate identified model. We were also able to reduce the order by introducing an input nonlinearity. Future work will focus on extracting other nonlinearities from the system, using the identified models to develop controllers for the isolator, and exploring the high displacement region of the capacitive displacement sensor.

References

[1] F. Ahmed-Zaid, P. A. Ioannou, and M. M. Polycarpou. Identification and control of aircraft dynamics using radial basis function networks. In *Second IEEE Confernce on Control Applications*, pages 567–572, Vancouver, BC, September 1993.

[2] E.-W. Bai. An optimal two-stage identification algorithm for Hammerstein-Wiener nonlinear systems. *Automatica*, 34(3):333–338, 1998.

[3] D. Bauer and B. Ninness. Asymptotic properties of least-squares estimates of Hammerstein-Wiener models. *International Journal of Control*, 75(1):34–51, 2002.

[4] D. S. Bayard and M. Eslami. Parameter identification of linear systems using nonlinear noninvertible measurements. In *Proceedings of the 23rd Conference on Decision and Control*, pages 348–352, Las Vegas, NV, December 1984.

[5] D. R. Brillinger. The identification of polynomial systems by means of higher order spectra. *Journal of Sound and Vibration*, 12(3):301–313, 1970.

[6] C. H. Chen and S. D. Fassois. Maximum likelihood identification of stochastic Wiener-Hammerstein-type non-linear systems. *Mechanical Systems and Signal Processing*, 6(2):135–153, 1992.

[7] S. Chen and S. A. Billings. Neural networks for nonlinear dynamic system modelling and identification. *International Journal of Control*, 56(2):319–346, 1992.

[8] S. Chen, S. A. Billings, C. F. N. Cowan, and P. M. Grant. Non-linear systems identification using radial basis functions. *International Journal of Systems Science*, 21(12):2513–2539, 1990.

[9] S. Chen, S. A. Billings, and P. M. Grant. Nonlinear system identification using neural networks. *International Journal of Control*, 51(6):1191–1214, 1990.

[10] H. E. Emara-Shabaik, K. A. F. Moustafa, and J. H. S. Talaq. On identification of parallel block-cascade nonlinear models. *International Journal of Systems Science*, 26(7):1429–1438, 1995.

[11] W. Greblicki. Nonparametric identification of Wiener systems by orthogonal series. *IEEE Transactions on Automatic Control*, 39(10):2077–2086, 1994.

[12] W. Greblicki. Nonparametric approach to Wiener system identification. *IEEE Transactions on Circuits and Systems – I: Fundamental Theory and Applications*, 44(6):538–545, 1997.

[13] R. Haber and L. Keviczky. *Nonlinear System Identification – Input-Output Modeling Approach*, volume 1: Nonlinear System Parameter Identification. Kluwer Academic Publishers, 1999.

[14] R. Haber and L. Keviczky. *Nonlinear System Identification – Input-Output Modeling Approach*, volume 2: Nonlinear System Structure Identification. Kluwer Academic Publishers, 1999.

[15] Z. Hasiewicz. Identification of a linear system observed through zero-memory non-linearity. *International Journal of Systems Science*, 18(9):1595–1607, 1987.

[16] I. W. Hunter and M. J. Korenberg. The identification of nonlinear biological systems: Wiener and Hammerstein cascade models. *Biological Cybernetics*, 55:135–144, 1986.

[17] Juditsky *et al*. Nonlinear black-box models in system identification: Mathematical foundations. *Automatica*, 31(12):1725–1750, 1995.

[18] M. J. Korenberg and I. W. Hunter. The identification of nonlinear biological systems: LNL cascade models. *Biological Cybernetics*, 55:125–134, 1986.

[19] S. L. Lacy and D. S. Bernstein. Subspace identification for nonlinear systems that are linear in unmeasured states. In *Proceedings of the Conference on Decision and Control*, Orlando, Florida, December 2001.

[20] S. L. Lacy and D. S. Bernstein. Identification of FIR Wiener systems with unknown, noninvertible, polynomial nonlinearities. In *Proceedings of the American Control Conference*, Anchorage, Alaska, May 2002.

[21] S. L. Lacy and D. S. Bernstein. Subspace identification with guaranteed stability using constrained optimization. In *Proceedings of the American Control Conference*, Anchorage, Alaska, May 2002.

[22] S. L. Lacy, R. S. Erwin, and D. S. Bernstein. Identification of Wiener systems with known noninvertible nonlinearities. *Journal of Dynamic Systems, Measurement, and Control*, 123:1–6, December 2001.

[23] M. Lovera, T. Gustafsson, and M. Verhaegen. Recursive subspace identification of linear and nonlinear Wiener state-space models. *Automatica*, 36:1639–1650, 2000.

[24] K. S. Narendra and K. Parthasarathy. Identification and control of dynamical systems using neural networks. *IEEE Transactions on Neural Networks*, 1(1):4–27, 1990.

[25] O. Nelles. *Nonlinear System Identification*. Springer, 2001.

[26] G. A. Pajunen. Recursive identification of Wiener type nonlinear systems. In *Proceedings of the 1985 American Control Conference*, volume 3, pages 1365–1370, Boston, MA, June 1985.

[27] Sjöberg *et al*. Nonlinear black-box modeling in system identification: A unified overview. *Automatica*, 31(12):1691–1724, 1995.

[28] T. Van Pelt and D. S. Bernstein. Nonlinear system identification using hammerstein and nonlinear feedback models with piecewise linear static maps - part I: Theory - part II: Numerical examples. In *Proceedings of the ACC*, pages 225 – 229, 235–239, Chicago, IL, June 2000.

[29] M. Verhaegen and D. Westwick. Identifying MIMO Hammerstein systems in the context of subspace model identification methods. *International Journal of Control*, 63(2):331–349, 1996.

[30] D. Westwick and M. Verhaegen. Identifying MIMO Wiener systems using subspace model identification methods. *Signal Processing*, 52:235–258, 1996.

[31] D. T. Westwick and R. E. Kearney. A new algorithm for the identification of multiple input Wiener systems. *Biological Cybernetics*, 68:75–85, 1992.

[32] T. Wigren. Convergence analysis of recursive identification algorithms based on the Wiener model. *IEEE Transactions on Automatic Control*, 39(11):2191–2206, 1994.